Contents

List of Figures

List of Tables

Chapter 9

Rigid Body Motion and Rotational Dynamics

9.1 Rigid Bodies

A rigid body consists of a group of particles whose separations are all fixed in magnitude. Six independent coordinates are required to completely specify the position and orientation of a rigid body. For example, the location of the first particle is specified by three coordinates. A second particle requires only two coordinates since the distance to the first is fixed. Finally, a third particle requires only one coordinate, since its distance to the first two particles is fixed (think about the intersection of two spheres). The positions of all the remaining particles are then determined by their distances from the first three. Usually, one takes these six coordinates to be the center-of-mass position $\boldsymbol{R} = (X, Y, Z)$ and three angles specifying the orientation of the body (*e.g.* the Euler angles).

As derived previously, the equations of motion are

$$\begin{aligned} \boldsymbol{P} = \sum_i m_i \, \dot{\boldsymbol{r}}_i \quad &, \quad \dot{\boldsymbol{P}} = \boldsymbol{F}^{(\rm ext)} \\ \boldsymbol{L} = \sum_i m_i \, \boldsymbol{r}_i \times \dot{\boldsymbol{r}}_i \quad &, \quad \dot{\boldsymbol{L}} = \boldsymbol{N}^{(\rm ext)} \quad . \end{aligned} \tag{9.1}$$

These equations determine the motion of a rigid body.

9.1.1 Examples of rigid bodies

Our first example of a rigid body is of a wheel rolling with constant angular velocity $\dot\phi = \omega$, and without slipping, This is shown in fig. 9.1. The no-slip condition is $dx = R\,d\phi$, so $\dot x = V_{\rm CM} = R\omega$. The velocity of a point within the wheel is

$$\boldsymbol{v} = \boldsymbol{V}_{\rm CM} + \boldsymbol{\omega} \times \boldsymbol{r} \quad , \tag{9.2}$$

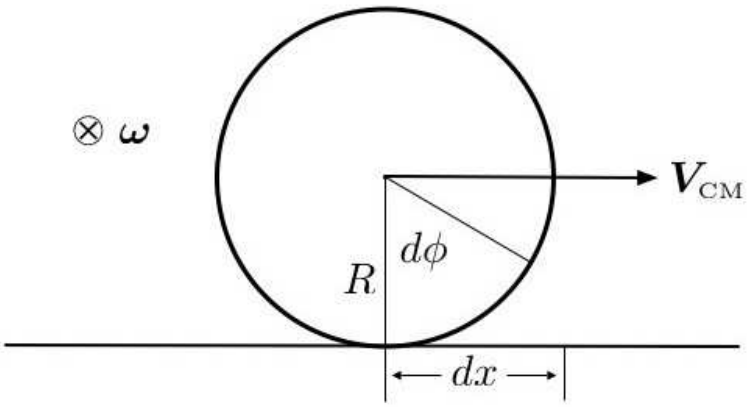

Figure 9.1: A wheel rolling to the right without slipping.

where $\boldsymbol{r}$ is measured from the center of the disk. The velocity of a point on the surface is then given by $\boldsymbol{v} = \omega R\big(\hat{\boldsymbol{x}} + \hat{\boldsymbol{\omega}} \times \hat{\boldsymbol{r}}\big)$.

As a second example, consider a bicycle wheel of mass M and radius R affixed to a light, firm rod of length d, as shown in fig. 9.2. Assuming $\boldsymbol{L}$ lies in the (x, y) plane, one computes the gravitational torque $\boldsymbol{N} = \boldsymbol{r} \times (M\boldsymbol{g}) = Mgd\,\hat{\boldsymbol{\phi}}$. The angular momentum vector then rotates with angular frequency $\dot{\phi}$. Thus,

$$d\phi = \frac{dL}{L} \quad \Longrightarrow \quad \dot{\phi} = \frac{Mgd}{L} \quad . \tag{9.3}$$

But $L = MR^2\omega$, so the precession frequency is

$$\omega_{\rm p} = \dot{\phi} = \frac{gd}{\omega R^2} \quad . \tag{9.4}$$

For $R = d = 30\,\text{cm}$ and $\omega/2\pi = 200\,\text{rpm}$, find $\omega_{\rm p}/2\pi \approx 15\,\text{rpm}$. Note that we have here ignored the contribution to $\boldsymbol{L}$ from the precession itself, which lies along $\hat{\boldsymbol{z}}$, resulting in the *nutation* of the wheel. This is justified if $L_{\rm p}/L = (d^2/R^2) \cdot (\omega_{\rm p}/\omega) \ll 1$.

9.2 The Inertia Tensor

Suppose first that a point within the body itself is fixed. This eliminates the translational degrees of freedom from consideration. We now have

$$\left(\frac{d\boldsymbol{r}}{dt}\right)_{\rm inertial} = \boldsymbol{\omega} \times \boldsymbol{r} \quad , \tag{9.5}$$

since $\dot{\boldsymbol{r}}_{\rm body} = 0$. The kinetic energy is then

$$\begin{aligned} T &= \tfrac{1}{2}\sum_i m_i \left(\frac{d\boldsymbol{r}_i}{dt}\right)^2_{\rm inertial} = \tfrac{1}{2}\sum_i m_i\,(\boldsymbol{\omega} \times \boldsymbol{r}_i) \cdot (\boldsymbol{\omega} \times \boldsymbol{r}_i) \\ &= \tfrac{1}{2}\sum_i m_i \Big[\omega^2\,\boldsymbol{r}_i^2 - (\boldsymbol{\omega} \cdot \boldsymbol{r}_i)^2\Big] \equiv \tfrac{1}{2} I_{\alpha\beta}\,\omega_\alpha\,\omega_\beta \quad , \end{aligned} \tag{9.6}$$

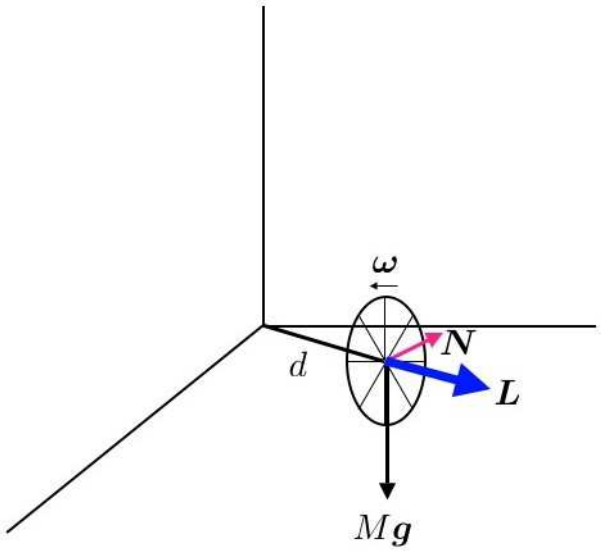

Figure 9.2: Precession of a spinning bicycle wheel.

where ω_α is the component of $\boldsymbol{\omega}$ along the body-fixed axis $\boldsymbol{e}_\alpha$. The quantity $I_{\alpha\beta}$ is the *inertia tensor,*

$$\begin{aligned} I_{\alpha\beta} &= \sum_i m_i \Big(\boldsymbol{r}_i^2 \, \delta_{\alpha\beta} - r_{i,\alpha} \, r_{i,\beta} \Big) \\ &= \int d^d r \, \varrho(\boldsymbol{r}) \left(\boldsymbol{r}^2 \, \delta_{\alpha\beta} - r_\alpha \, r_\beta \right) \quad \text{(continuous media)} \quad . \end{aligned} \tag{9.7}$$

The angular momentum is

$$\begin{aligned} \boldsymbol{L} &= \sum_i m_i \, \boldsymbol{r}_i \times \left(\frac{d\boldsymbol{r}_i}{dt} \right)_{\text{inertial}} \\ &= \sum_i m_i \, \boldsymbol{r}_i \times (\boldsymbol{\omega} \times \boldsymbol{r}_i) = I_{\alpha\beta} \, \omega_\beta \quad . \end{aligned} \tag{9.8}$$

The diagonal elements of $I_{\alpha\beta}$ are called the *moments of inertia*, while the off-diagonal elements are called the *products of inertia.*

9.2.1 Coordinate transformations

Consider the basis transformation

$$\hat{\mathbf{e}}'_\alpha = \mathcal{R}_{\alpha\beta} \, \hat{\mathbf{e}}_\beta \quad . \tag{9.9}$$

We demand $\hat{\mathbf{e}}'_\alpha \cdot \hat{\mathbf{e}}'_\beta = \delta_{\alpha\beta}$, which means $\mathcal{R} \in \mathrm{O}(d)$ is an orthogonal matrix, *i.e.* $\mathcal{R}^{\mathrm{t}} = \mathcal{R}^{-1}$. Thus the inverse transformation is $\boldsymbol{e}_\alpha = \mathcal{R}^{\mathrm{t}}_{\alpha\beta} \boldsymbol{e}'_\beta$. Consider next a general vector $\boldsymbol{A} = A_\beta \, \hat{\mathbf{e}}_\beta$. Expressed in terms of the new basis $\{\hat{\mathbf{e}}'_\alpha\}$, we have

$$\boldsymbol{A} = A_\beta \, \overbrace{\mathcal{R}^{\mathrm{t}}_{\beta\alpha} \, \hat{\mathbf{e}}'_\alpha}^{\hat{\mathbf{e}}_\beta} = \overbrace{\mathcal{R}_{\alpha\beta} A_\beta}^{A'_\alpha} \, \hat{\mathbf{e}}'_\alpha \tag{9.10}$$

Thus, the components of $\boldsymbol{A}$ transform as $A'_\alpha = \mathcal{R}_{\alpha\beta}\, A_\beta$. This is true for any vector.

Under a rotation, the density $\rho(\boldsymbol{r})$ must satisfy $\rho'(\boldsymbol{r}') = \rho(\boldsymbol{r})$. This is the transformation rule for scalars. The inertia tensor therefore obeys

$$\begin{aligned} I'_{\alpha\beta} &= \int d^3r'\, \rho'(\boldsymbol{r}') \left[\boldsymbol{r}'^2\, \delta_{\alpha\beta} - r'_\alpha\, r'_\beta \right] \\ &= \int d^3r\, \rho(\boldsymbol{r}) \left[\boldsymbol{r}^2\, \delta_{\alpha\beta} - \big(\mathcal{R}_{\alpha\mu} r_\mu\big)\big(\mathcal{R}_{\beta\nu} r_\nu\big) \right] \\ &= \mathcal{R}_{\alpha\mu}\, I_{\mu\nu}\, \mathcal{R}^{\rm t}_{\nu\beta} \quad . \end{aligned} \tag{9.11}$$

I.e. $I' = \mathcal{R} I \mathcal{R}^{\rm t}$, the transformation rule for tensors. The angular frequency $\boldsymbol{\omega}$ is a vector, so $\omega'_\alpha = \mathcal{R}_{\alpha\mu}\, \omega_\mu$. The angular momentum $\boldsymbol{L}$ also transforms as a vector. The kinetic energy is $T = \frac{1}{2}\, \boldsymbol{\omega}^{\rm t} \cdot I \cdot \boldsymbol{\omega}$, which transforms as a scalar.

9.2.2 The case of no fixed point

If there is no fixed point, we can let $\boldsymbol{r}'$ denote the distance from the center-of-mass (CM), which will serve as the instantaneous origin in the body-fixed frame. We then adopt the notation where $\boldsymbol{R}$ is the CM position of the rotating body, as observed in an inertial frame, and is computed from the expression

$$\boldsymbol{R} = \frac{1}{M} \sum_i m_i\, \boldsymbol{\rho}_i = \frac{1}{M} \int d^3r\, \rho(\boldsymbol{r})\, \boldsymbol{r} \quad , \tag{9.12}$$

where the total mass is of course

$$M = \sum_i m_i = \int d^3r\, \rho(\boldsymbol{r}) \quad . \tag{9.13}$$

The kinetic energy and angular momentum are then

$$\begin{aligned} T &= \tfrac{1}{2} M \dot{\boldsymbol{R}}^2 + \tfrac{1}{2} I_{\alpha\beta}\, \omega_\alpha\, \omega_\beta \\ L_\alpha &= \epsilon_{\alpha\beta\gamma} M R_\beta \dot{R}_\gamma + I_{\alpha\beta}\, \omega_\beta \quad , \end{aligned} \tag{9.14}$$

where $I_{\alpha\beta}$ is given in eqs. 9.7, where the origin is the CM.

9.3 Parallel Axis Theorem

Suppose $I_{\alpha\beta}$ is given in a body-fixed frame. If we displace the origin in the body-fixed frame by $\boldsymbol{d}$, then let $I_{\alpha\beta}(\boldsymbol{d})$ be the inertial tensor with respect to the new origin. If, relative to the origin at $\boldsymbol{0}$ a mass element lies at position $\boldsymbol{r}$, then relative to an origin at $\boldsymbol{d}$ it will lie at $\boldsymbol{r} - \boldsymbol{d}$. We then have

$$I_{\alpha\beta}(\boldsymbol{d}) = \sum_i m_i \Big\{ (\boldsymbol{r}_i^2 - 2\boldsymbol{d}\cdot\boldsymbol{r}_i + \boldsymbol{d}^2)\, \delta_{\alpha\beta} - (r_{i,\alpha} - d_\alpha)(r_{i,\beta} - d_\beta) \Big\} \quad . \tag{9.15}$$

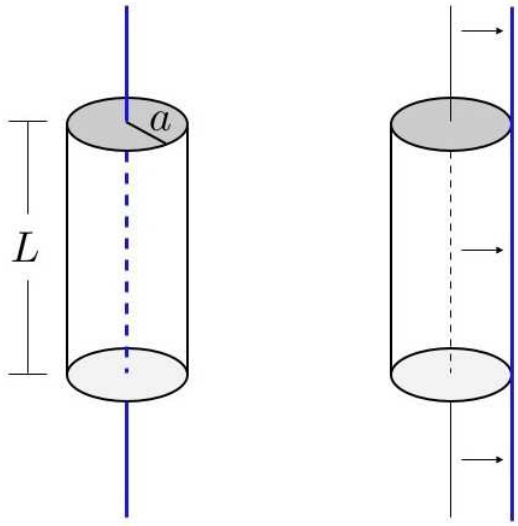

Figure 9.3: Application of the parallel axis theorem to a cylindrically symmetric mass distribution.

If $\boldsymbol{r}_i$ is measured with respect to the CM, then

$$\sum_i m_i \, \boldsymbol{r}_i = 0 \tag{9.16}$$

and

$$I_{\alpha\beta}(\boldsymbol{d}) = I_{\alpha\beta}(0) + M\big(\boldsymbol{d}^2\delta_{\alpha\beta} - d_\alpha d_\beta\big) \quad , \tag{9.17}$$

a result known as the *parallel axis theorem.*

As an example of the theorem, consider the situation depicted in fig. 9.3, where a cylindrically symmetric mass distribution is rotated about is symmetry axis, and about an axis tangent to its side. The component I_{zz} of the inertia tensor is easily computed when the origin lies along the symmetry axis:

$$\begin{aligned} I_{zz} &= \int d^3r\,\rho(\boldsymbol{r})\,(\boldsymbol{r}^2 - z^2) = \rho L\cdot 2\pi\int_0^a dr_\perp\, r_\perp^3 \\ &= \tfrac{\pi}{2}\rho L a^4 = \tfrac{1}{2}Ma^2 \quad , \end{aligned} \tag{9.18}$$

where $M = \pi a^2 L\rho$ is the total mass. If we compute I_{zz} about a vertical axis which is tangent to the cylinder, the parallel axis theorem tells us that

$$I'_{zz} = I_{zz} + Ma^2 = \tfrac{3}{2}Ma^2 \quad . \tag{9.19}$$

Doing this calculation by explicit integration of $\int dm\, r_\perp^2$ would be tedious!

9.3.1 Example

Problem: Compute the CM and the inertia tensor for the planar right triangle of fig. 9.4, assuming it to be of uniform two-dimensional mass density ρ.

Solution: The total mass is $M = \frac{1}{2}\rho\, ab$. The x-coordinate of the CM is then

$$\begin{aligned} X &= \frac{1}{M}\int\limits_0^a dx \int\limits_0^{b(1-\frac{x}{a})} dy\, \rho\, x = \frac{\rho}{M}\int\limits_0^a dx\, b\big(1-\tfrac{x}{a}\big)\, x \\ &= \frac{\rho\, a^2 b}{M}\int\limits_0^1 du\, u(1-u) = \frac{\rho\, a^2 b}{6M} = \tfrac{1}{3}\, a \quad . \end{aligned} \tag{9.20}$$

Clearly we must then have $Y = \frac{1}{3}\, b$, which may be verified by explicit integration.

We now compute the inertia tensor, with the origin at $(0, 0, 0)$. Since the figure is planar, $z = 0$ everywhere, hence $I_{xz} = I_{zx} = 0$, $I_{yz} = I_{zy} = 0$, and also $I_{zz} = I_{xx} + I_{yy}$. We now compute the remaining independent elements:

$$\begin{aligned} I_{xx} &= \rho\int\limits_0^a dx \int\limits_0^{b(1-\frac{x}{a})} dy\, y^2 = \rho\int\limits_0^a dx\, \tfrac{1}{3}\, b^3\, \big(1-\tfrac{x}{a}\big)^3 \\ &= \tfrac{1}{3}\rho\, ab^3\int\limits_0^1 du\, (1-u)^3 = \tfrac{1}{12}\rho\, ab^3 = \tfrac{1}{6}Mb^2 \end{aligned} \tag{9.21}$$

and

$$\begin{aligned} I_{xy} &= -\rho\int\limits_0^a dx \int\limits_0^{b(1-\frac{x}{a})} dy\, x\, y = -\tfrac{1}{2}\rho\, b^2\int\limits_0^a dx\, x\, \big(1-\tfrac{x}{a}\big)^2 \\ &= -\tfrac{1}{2}\rho\, a^2 b^2\int\limits_0^1 du\, u\, (1-u)^2 = -\tfrac{1}{24}\rho\, a^2 b^2 = -\tfrac{1}{12}Mab \quad . \end{aligned} \tag{9.22}$$

Thus,

$$I = \frac{M}{6}\begin{pmatrix} b^2 & -\frac{1}{2}ab & 0 \\ -\frac{1}{2}ab & a^2 & 0 \\ 0 & 0 & a^2+b^2 \end{pmatrix} \quad . \tag{9.23}$$

Suppose we wanted the inertia tensor relative in a coordinate system where the CM lies at the origin. What we computed in eqn. 9.23 is $I(\boldsymbol{d})$, with $\boldsymbol{d} = -\frac{a}{3}\hat{\boldsymbol{x}} - \frac{b}{3}\,\hat{\boldsymbol{y}}$. Thus,

$$\boldsymbol{d}^2\delta_{\alpha\beta} - d_\alpha\, d_\beta = \frac{1}{9}\begin{pmatrix} b^2 & -ab & 0 \\ -ab & a^2 & 0 \\ 0 & 0 & a^2+b^2 \end{pmatrix} \quad . \tag{9.24}$$

Since

$$I(\boldsymbol{d}) = I^{\rm CM} + M\Big(\boldsymbol{d}^2\delta_{\alpha\beta} - d_\alpha\, d_\beta\Big) \quad , \tag{9.25}$$

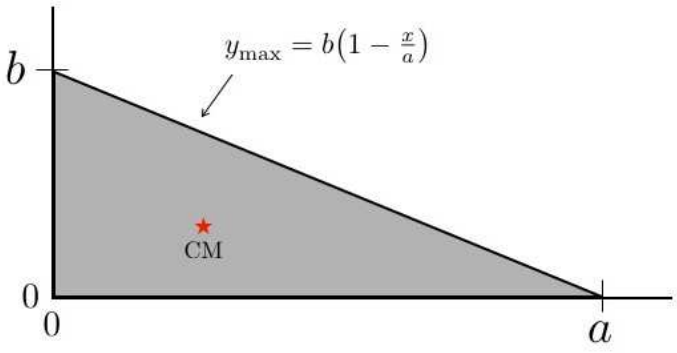

Figure 9.4: A planar mass distribution in the shape of a triangle.

we have that

$$I^{\rm CM} = I(\boldsymbol{d}) - M\Big(\boldsymbol{d}^2\delta_{\alpha\beta} - d_\alpha\, d_\beta\Big) = \frac{M}{18}\begin{pmatrix} b^2 & \frac{1}{2}ab & 0 \\ \frac{1}{2}ab & a^2 & 0 \\ 0 & 0 & a^2+b^2 \end{pmatrix} \quad . \tag{9.26}$$

9.3.2 General planar mass distribution

For a general planar mass distribution,

$$\rho(x,y,z) = \sigma(x,y)\,\delta(z) \quad , \tag{9.27}$$

which is confined to the plane $z = 0$, we have $I_{xz} = I_{yz} = 0$, and

$$\begin{aligned} I_{xx} &= \int dx \int dy\, \sigma(x,y)\, y^2 \\ I_{yy} &= \int dx \int dy\, \sigma(x,y)\, x^2 \\ I_{xy} &= -\int dx \int dy\, \sigma(x,y)\, xy \quad . \end{aligned} \tag{9.28}$$

Furthermore, $I_{zz} = I_{xx} + I_{yy}$, regardless of the two-dimensional mass distribution $\sigma(x,y)$.

9.4 Principal Axes of Inertia

We found that an orthogonal transformation to a new set of axes $\hat{\mathbf{e}}'_\alpha = \mathcal{R}_{\alpha\beta}\hat{\mathbf{e}}_\beta$ entails $I' = \mathcal{R}I\mathcal{R}^{\rm t}$ for the inertia tensor. Since $I = I^{\rm t}$ is manifestly a symmetric matrix, it can be brought to diagonal form by such an orthogonal transformation. To find $\mathcal{R}$, follow this recipe:

1. Find the diagonal elements of I' by setting $P(\lambda) = 0$, where

$$P(\lambda) = \det\big(\lambda \cdot 1 - I\big) \quad , \tag{9.29}$$

   is the characteristic polynomial for I, and 1 is the unit matrix.

2. For each eigenvalue λ_a, solve the d equations

$$\sum_\nu I_{\mu\nu}\,\psi^a_\nu = \lambda_a\,\psi^a_\mu \quad . \tag{9.30}$$

   Here, ψ^a_μ is the $\mu^{\rm th}$ component of the $a^{\rm th}$ eigenvector. Since $(\lambda \cdot 1 - I)$ is degenerate, these equations are linearly dependent, which means that the first $d-1$ components may be determined in terms of the $d^{\rm th}$ component.

3. Because $I = I^{\rm t}$, eigenvectors corresponding to different eigenvalues are orthogonal. In cases of degeneracy, the eigenvectors may be chosen to be orthogonal, *e.g.* via the Gram-Schmidt procedure.

4. Due to the underdetermined aspect to step 2, we may choose an arbitrary normalization for each eigenvector. It is conventional to choose the eigenvectors to be orthonormal: $\sum_\mu \psi^a_\mu\,\psi^b_\mu = \delta^{ab}$.

5. The matrix $\mathcal{R}$ is explicitly given by $\mathcal{R}_{a\mu} = \psi^a_\mu$, the matrix whose row vectors are the eigenvectors $\boldsymbol{\psi}^a$. Of course $\mathcal{R}^{\rm t}$ is then the corresponding matrix of column vectors.

6. The eigenvectors form a complete basis. The resolution of unity may be expressed as

$$\sum_a \psi^a_\mu\,\psi^a_\nu = \delta_{\mu\nu} \quad . \tag{9.31}$$

As an example, consider the inertia tensor for a general planar mass distribution, which is of the form

$$I = \begin{pmatrix} I_{xx} & I_{xy} & 0 \\ I_{yx} & I_{yy} & 0 \\ 0 & 0 & I_{zz} \end{pmatrix} \quad , \tag{9.32}$$

where $I_{yx} = I_{xy}$ and $I_{zz} = I_{xx} + I_{yy}$. Define

$$\begin{aligned} A &= \tfrac{1}{2}\big(I_{xx} + I_{yy}\big) \\ B &= \sqrt{\tfrac{1}{4}\big(I_{xx} - I_{yy}\big)^2 + I_{xy}^2} \\ \vartheta &= \tan^{-1}\left(\frac{2I_{xy}}{I_{xx} - I_{yy}}\right) \quad , \end{aligned} \tag{9.33}$$

so that

$$I = \begin{pmatrix} A + B\cos\vartheta & B\sin\vartheta & 0 \\ B\sin\vartheta & A - B\cos\vartheta & 0 \\ 0 & 0 & 2A \end{pmatrix} \quad , \tag{9.34}$$

The characteristic polynomial is found to be

$$P(\lambda) = (\lambda - 2A)\left[(\lambda - A)^2 - B^2\right] \quad , \tag{9.35}$$

which gives $\lambda_1 = A + B$, $\lambda_2 = A - B$, and $\lambda_3 = 2A$. The corresponding normalized eigenvectors are

$$\boldsymbol{\psi}^1 = \begin{pmatrix} \cos\frac{1}{2}\vartheta \\ \sin\frac{1}{2}\vartheta \\ 0 \end{pmatrix} \quad , \quad \boldsymbol{\psi}^2 = \begin{pmatrix} -\sin\frac{1}{2}\vartheta \\ \cos\frac{1}{2}\vartheta \\ 0 \end{pmatrix} \quad , \quad \boldsymbol{\psi}^3 = \begin{pmatrix} 0 \\ 0 \\ 1 \end{pmatrix} \tag{9.36}$$

and therefore

$$\mathcal{R} = \begin{pmatrix} \cos\frac{1}{2}\vartheta & \sin\frac{1}{2}\vartheta & 0 \\ -\sin\frac{1}{2}\vartheta & \cos\frac{1}{2}\vartheta & 0 \\ 0 & 0 & 1 \end{pmatrix} \quad . \tag{9.37}$$

We then have

$$I' = \mathcal{R} I \mathcal{R}^{\rm t} = \begin{pmatrix} A+B & 0 & 0 \\ 0 & A-B & 0 \\ 0 & 0 & 2A \end{pmatrix} \quad . \tag{9.38}$$

9.5 Euler's Equations

9.5.1 Derivation of Euler's equations

The equations of motion are

$$\begin{aligned} \boldsymbol{N}^{\rm ext} &= \left(\frac{d\boldsymbol{L}}{dt}\right)_{\rm inertial} \\ &= \left(\frac{d\boldsymbol{L}}{dt}\right)_{\rm body} + \boldsymbol{\omega} \times \boldsymbol{L} = I\dot{\boldsymbol{\omega}} + \boldsymbol{\omega} \times (I\boldsymbol{\omega}) \quad . \end{aligned} \tag{9.39}$$

Let us now choose our coordinate axes to be the principal axes of inertia, with the CM at the origin. We may then write

$$\boldsymbol{\omega} = \begin{pmatrix} \omega_1 \\ \omega_2 \\ \omega_3 \end{pmatrix} \quad , \quad I = \begin{pmatrix} I_1 & 0 & 0 \\ 0 & I_2 & 0 \\ 0 & 0 & I_3 \end{pmatrix} \quad \Longrightarrow \quad \boldsymbol{L} = \begin{pmatrix} I_1\,\omega_1 \\ I_2\,\omega_2 \\ I_3\,\omega_3 \end{pmatrix} \quad . \tag{9.40}$$

From $I\dot{\boldsymbol{\omega}} + \boldsymbol{\omega} \times (I\boldsymbol{\omega}) = \boldsymbol{N}^{\rm ext}$, we arrive at *Euler's equations:*

$$\begin{aligned} I_1\,\dot{\omega}_1 &= (I_2 - I_3)\,\omega_2\,\omega_3 + N_1^{\rm ext} \\ I_2\,\dot{\omega}_2 &= (I_3 - I_1)\,\omega_3\,\omega_1 + N_2^{\rm ext} \\ I_3\,\dot{\omega}_3 &= (I_1 - I_2)\,\omega_1\,\omega_2 + N_3^{\rm ext} \quad , \end{aligned} \tag{9.41}$$

where $N^{\rm ext}_{1,2,3}$ are the components of $\boldsymbol{N}^{\rm ext}$ along the body-fixed principal axes. These equations are coupled and nonlinear. We can however make progress in the case where $\boldsymbol{N}^{\rm ext} = 0$, *i.e.* when there are no

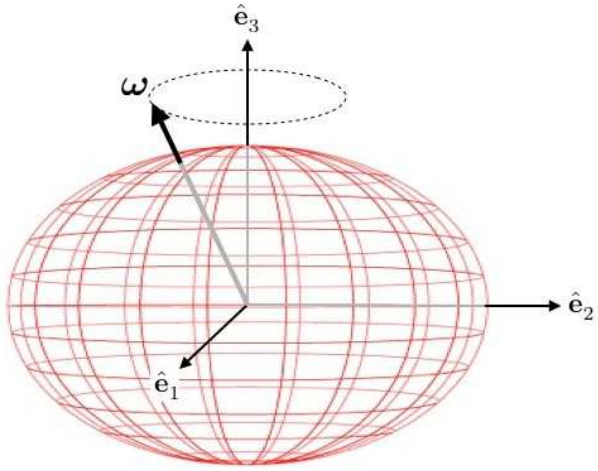

Figure 9.5: Wobbling of a torque-free symmetric top.

external torques. This is true for a body in free space, or in a uniform gravitational field. In the latter case,

$$\boldsymbol{N}^{\rm ext} = \sum_i \boldsymbol{r}_i \times (m_i\,\boldsymbol{g}) = \Big(\sum_i m_i \boldsymbol{r}_i\Big) \times \boldsymbol{g} \quad , \tag{9.42}$$

where $\boldsymbol{g}$ is the uniform gravitational acceleration. In a body-fixed frame whose origin is the CM, we have $\sum_i m_i \boldsymbol{r}_i = 0$, and the external torque vanishes!

9.5.2 Precession of torque-free symmetric tops

Consider a body which has a symmetry axis $\hat{\mathbf{e}}_3$. This guarantees $I_1 = I_2$, but in general we still have $I_1 \neq I_3$. In the absence of external torques, the last of Euler's equations says $\dot\omega_3 = 0$, so ω_3 is a constant. The remaining two equations are then

$$\dot\omega_1 = \left(\frac{I_1 - I_3}{I_1}\right)\omega_3\,\omega_2 \quad , \quad \dot\omega_2 = \left(\frac{I_3 - I_1}{I_1}\right)\omega_3\,\omega_1 \quad . \tag{9.43}$$

I.e. $\dot\omega_1 = -\Omega\,\omega_2$ and $\dot\omega_2 = +\Omega\,\omega_1$, with

$$\Omega = \left(\frac{I_3 - I_1}{I_1}\right)\omega_3 \quad , \tag{9.44}$$

which are the equations of a harmonic oscillator. The solution is easily obtained:

$$\omega_1(t) = \omega_\perp \cos\big(\Omega t + \delta\big) \quad , \quad \omega_2(t) = \omega_\perp \sin\big(\Omega t + \delta\big) \quad , \quad \omega_3(t) = \omega_3 \quad , \tag{9.45}$$

where $\omega_\perp$ and δ are constants of integration, and where $|\boldsymbol{\omega}| = (\omega_\perp^2 + \omega_3^2)^{1/2}$. This motion is sketched in fig. 9.5. Note that the perpendicular components of $\boldsymbol{\omega}$ oscillate harmonically, and that the angle $\boldsymbol{\omega}$ makes with respect to $\hat{\mathbf{e}}_3$ is $\lambda = \tan^{-1}(\omega_\perp/\omega_3)$.

For the earth, $(I_3 - I_1)/I_1 \approx \frac{1}{305}$ and $\omega_\perp \ll \omega_3$, so $\Omega \approx \omega/305$, *i.e.* a precession period of 305 days, or roughly 10 months. Astronomical observations reveal such a precession, known as the *Chandler wobble*. The precession angle is $\lambda_{\rm Chandler} \simeq 6 \times 10^{-7}$ rad, which means that the North Pole moves by about 4 meters during the wobble. The Chandler wobble has a period of about 14 months, so the naïve prediction of 305 days is off by a substantial amount. This discrepancy is attributed to the mechanical properties of the earth: elasticity and fluidity. The earth is not solid![1]

9.5.3 Asymmetric tops

Next, consider the torque-free motion of an asymmetric top, where $I_1 \neq I_2 \neq I_3 \neq I_1$. Unlike the symmetric case, there is no conserved component of $\boldsymbol{\omega}$. True, we can invoke conservation of energy and angular momentum,

$$\begin{aligned} E &= \tfrac{1}{2} I_1\,\omega_1^2 + \tfrac{1}{2} I_2\,\omega_2^2 + \tfrac{1}{2} I_3\,\omega_3^2 \\ \boldsymbol{L}^2 &= I_1^2\,\omega_1^2 + I_2^2\,\omega_2^2 + I_3^2\,\omega_3^2 \quad , \end{aligned} \tag{9.46}$$

and, in principle, solve for ω_1 and ω_2 in terms of ω_3, and then invoke Euler's equations (which must honor these conservation laws). This results in a nonlinear first order ODE of the form $\dot\omega_3 = f(\omega_3)$ which is fairly awkward.

We can, however, find a *particular* solution quite easily – one in which the rotation is about a single axis. Thus, $\omega_1 = \omega_2 = 0$ and $\omega_3 = \omega_0$ is indeed a solution for all time, according to Euler's equations. Let us now perturb about this solution, to explore its stability. We write

$$\boldsymbol{\omega} = \omega_0\,\hat{\mathbf{e}}_3 + \delta\boldsymbol{\omega} \quad , \tag{9.47}$$

and we invoke Euler's equations, linearizing by dropping terms quadratic in $\delta\boldsymbol{\omega}$. This yield

$$\begin{aligned} I_1\,\delta\dot\omega_1 &= (I_2 - I_3)\,\omega_0\,\delta\omega_2 + \mathcal{O}(\delta\omega_2\,\delta\omega_3) \\ I_2\,\delta\dot\omega_2 &= (I_3 - I_1)\,\omega_0\,\delta\omega_1 + \mathcal{O}(\delta\omega_3\,\delta\omega_1) \\ I_3\,\delta\dot\omega_3 &= 0 + \mathcal{O}(\delta\omega_1\,\delta\omega_2) \quad . \end{aligned} \tag{9.48}$$

Taking the time derivative of the first equation and invoking the second, and *vice versa*, yields

$$\delta\ddot\omega_1 = -\Omega^2\,\delta\omega_1 \quad , \quad \delta\ddot\omega_2 = -\Omega^2\,\delta\omega_2 \quad , \tag{9.49}$$

with

$$\Omega^2 = \frac{(I_3 - I_2)(I_3 - I_1)}{I_1\,I_2} \cdot \omega_0^2 \quad . \tag{9.50}$$

The solution is then $\delta\omega_1(t) = C\,\cos(\Omega t + \delta)$.

If $\Omega^2 > 0$, then Ω is real, and the deviation results in a harmonic precession. This occurs if I_3 is either the largest or the smallest of the moments of inertia. If, however, I_3 is the middle moment, then $\Omega^2 < 0$, and Ω is purely imaginary. The perturbation will in general increase exponentially with time, which means that the initial solution to Euler's equations is *unstable* with respect to small perturbations. This result can be vividly realized using a tennis racket, and sometimes goes by the name of the "tennis racket theorem."

[1] The earth is a layered like a *Mozartkugel*, with a solid outer shell, an inner fluid shell, and a solid (iron) core.

9.5.4 Example: The giant asteroid

PROBLEM: A unsuspecting solid spherical planet of mass M_0 rotates with angular velocity ω_0. Suddenly, a giant asteroid of mass αM_0 smashes into and sticks to the planet at a location which is at polar angle θ relative to the initial rotational axis. The new mass distribution is no longer spherically symmetric, and the rotational axis will precess. Recall Euler's equation,

$$\frac{d\boldsymbol{L}}{dt} + \boldsymbol{\omega} \times \boldsymbol{L} = \boldsymbol{N}^{\rm ext} \tag{9.51}$$

for rotations in a body-fixed frame.

(a) What is the new inertia tensor $I_{\alpha\beta}$ along principal center-of-mass frame axes? Don't forget that the CM is no longer at the center of the sphere! Recall $I = \frac{2}{5}MR^2$ for a solid sphere.

(b) What is the period of precession of the rotational axis in terms of the original length of the day $2\pi/\omega_0$?

SOLUTION: Let's choose body-fixed axes with $\hat{\boldsymbol{z}}$ pointing from the center of the planet to the smoldering asteroid. The CM lies a distance

$$d = \frac{\alpha M_0 \cdot R + M_0 \cdot 0}{(1+\alpha)M_0} = \frac{\alpha}{1+\alpha}\,R \tag{9.52}$$

from the center of the sphere. Thus, relative to the center of the sphere, we have

$$I = \tfrac{2}{5}M_0R^2 \begin{pmatrix} 1 & 0 & 0 \\ 0 & 1 & 0 \\ 0 & 0 & 1 \end{pmatrix} + \alpha M_0 R^2 \begin{pmatrix} 1 & 0 & 0 \\ 0 & 1 & 0 \\ 0 & 0 & 0 \end{pmatrix} \quad . \tag{9.53}$$

Now we shift to a frame with the CM at the origin, using the parallel axis theorem,

$$I_{\alpha\beta}(\boldsymbol{d}) = I^{\rm CM}_{\alpha\beta} + M\big(\boldsymbol{d}^2\,\delta_{\alpha\beta} - d_\alpha d_\beta\big) \quad . \tag{9.54}$$

Thus, with $\boldsymbol{d} = d\hat{\boldsymbol{z}}$,

$$\begin{aligned} I^{\rm CM}_{\alpha\beta} &= \tfrac{2}{5}M_0R^2 \begin{pmatrix} 1 & 0 & 0 \\ 0 & 1 & 0 \\ 0 & 0 & 1 \end{pmatrix} + \alpha M_0 R^2 \begin{pmatrix} 1 & 0 & 0 \\ 0 & 1 & 0 \\ 0 & 0 & 0 \end{pmatrix} - (1+\alpha)M_0 d^2 \begin{pmatrix} 1 & 0 & 0 \\ 0 & 1 & 0 \\ 0 & 0 & 0 \end{pmatrix} \\ &= M_0R^2 \begin{pmatrix} \frac{2}{5} + \frac{\alpha}{1+\alpha} & 0 & 0 \\ 0 & \frac{2}{5} + \frac{\alpha}{1+\alpha} & 0 \\ 0 & 0 & \frac{2}{5} \end{pmatrix} \quad . \end{aligned} \tag{9.55}$$

In the absence of external torques, Euler's equations along principal axes read

$$\begin{aligned} I_1 \frac{d\omega_1}{dt} &= (I_2 - I_3)\,\omega_2\,\omega_3 \\ I_2 \frac{d\omega_2}{dt} &= (I_3 - I_1)\,\omega_3\,\omega_1 \\ I_3 \frac{d\omega_3}{dt} &= (I_1 - I_2)\,\omega_1\,\omega_2 \end{aligned} \tag{9.56}$$

Since $I_1 = I_2$, $\omega_3(t) = \omega_3(0) = \omega_0 \cos\theta$ is a constant. We then obtain $\dot\omega_1 = \Omega\omega_2$, and $\dot\omega_2 = -\Omega\omega_1$, with

$$\Omega = \frac{I_2 - I_3}{I_1}\,\omega_3 = \frac{5\alpha}{7\alpha+2}\,\omega_3 \quad . \tag{9.57}$$

The period of precession τ in units of the pre-cataclysmic day is

$$\frac{\tau}{T} = \frac{\omega}{\Omega} = \frac{7\alpha+2}{5\alpha\cos\theta} \quad . \tag{9.58}$$

9.6 Euler's Angles

9.6.1 Definition of the Euler angles

In d dimensions, an orthogonal matrix $\mathcal{R} \in \mathrm{O}(d)$ has $\frac{1}{2}d(d-1)$ independent parameters. To see this, consider the constraint $\mathcal{R}^{\rm t}\mathcal{R} = 1$. The matrix $\mathcal{R}^{\rm t}\mathcal{R}$ is manifestly symmetric, so it has $\frac{1}{2}d(d+1)$ independent entries (*e.g.* on the diagonal and above the diagonal). This amounts to $\frac{1}{2}d(d+1)$ constraints on the d^2 components of $\mathcal{R}$, resulting in $\frac{1}{2}d(d-1)$ freedoms. Thus, in $d = 3$ rotations are specified by three parameters. The *Euler angles* $\{\phi, \theta, \psi\}$ provide one such convenient parameterization.

A general rotation $\mathcal{R}(\phi,\theta,\psi)$ is built up in three steps. We start with an orthonormal triad $\hat{\mathbf{e}}^0_\mu$ of body-fixed axes. The first step is a rotation by an angle ϕ about $\hat{\mathbf{e}}^0_3$:

$$\hat{\mathbf{e}}'_\mu = \mathcal{R}_{\mu\nu}\big(\hat{\mathbf{e}}^0_3, \phi\big)\,\hat{\mathbf{e}}^0_\nu \quad , \quad \mathcal{R}\big(\hat{\mathbf{e}}^0_3,\phi\big) = \begin{pmatrix} \cos\phi & \sin\phi & 0 \\ -\sin\phi & \cos\phi & 0 \\ 0 & 0 & 1 \end{pmatrix} \quad . \tag{9.59}$$

This step is shown in panel (a) of fig. 9.6. The second step is a rotation by θ about the new axis $\hat{\mathbf{e}}'_1$:

$$\hat{\mathbf{e}}''_\mu = \mathcal{R}_{\mu\nu}\big(\hat{\mathbf{e}}'_1, \theta\big)\,\hat{\mathbf{e}}'_\nu \quad , \quad \mathcal{R}\big(\hat{\mathbf{e}}'_1,\theta\big) = \begin{pmatrix} 1 & 0 & 0 \\ 0 & \cos\theta & \sin\theta \\ 0 & -\sin\theta & \cos\theta \end{pmatrix} \quad . \tag{9.60}$$

This step is shown in panel (b). The third and final step is a rotation by ψ about the new axis $\hat{\mathbf{e}}''_3$:

$$\hat{\mathbf{e}}'''_\mu = \mathcal{R}_{\mu\nu}\big(\hat{\mathbf{e}}''_3, \psi\big)\,\hat{\mathbf{e}}''_\nu \quad , \quad \mathcal{R}\big(\hat{\mathbf{e}}''_3,\psi\big) = \begin{pmatrix} \cos\psi & \sin\psi & 0 \\ -\sin\psi & \cos\psi & 0 \\ 0 & 0 & 1 \end{pmatrix} \quad . \tag{9.61}$$

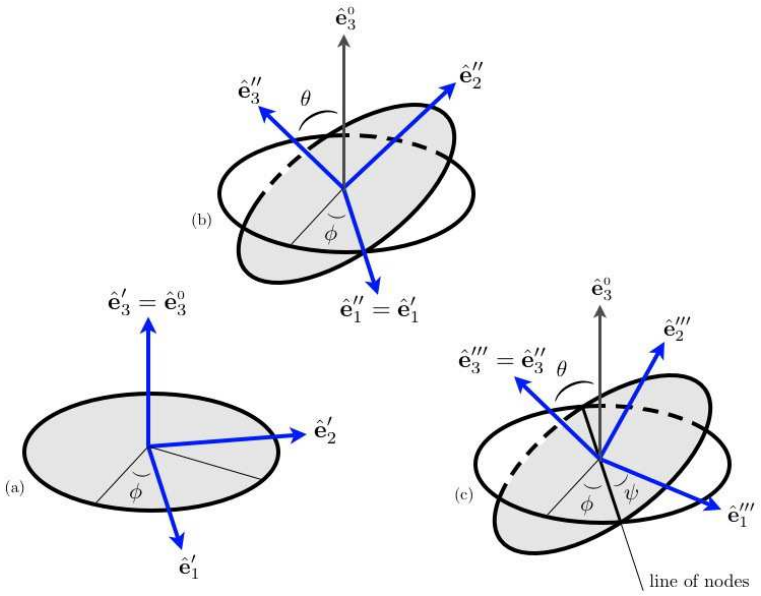

Figure 9.6: A general rotation, defined in terms of the Euler angles $\{\phi, \theta, \psi\}$. Three successive steps of the transformation are shown.

This step is shown in panel (c). Putting this all together,

$$\mathcal{R}(\phi,\theta,\psi) = \mathcal{R}\big(\hat{\mathbf{e}}_3'',\psi\big)\,\mathcal{R}\big(\hat{\mathbf{e}}_1',\theta\big)\,\mathcal{R}\big(\hat{\mathbf{e}}_3^0,\phi\big) \tag{9.62}$$

$$= \begin{pmatrix} \cos\psi & \sin\psi & 0 \\ -\sin\psi & \cos\psi & 0 \\ 0 & 0 & 1 \end{pmatrix} \begin{pmatrix} 1 & 0 & 0 \\ 0 & \cos\theta & \sin\theta \\ 0 & -\sin\theta & \cos\theta \end{pmatrix} \begin{pmatrix} \cos\phi & \sin\phi & 0 \\ -\sin\phi & \cos\phi & 0 \\ 0 & 0 & 1 \end{pmatrix}$$

$$= \begin{pmatrix} \cos\psi\cos\phi - \sin\psi\cos\theta\sin\phi & \cos\psi\sin\phi + \sin\psi\cos\theta\cos\phi & \sin\psi\sin\theta \\ -\sin\psi\cos\phi - \cos\psi\cos\theta\sin\phi & -\sin\psi\sin\phi + \cos\psi\cos\theta\cos\phi & \cos\psi\sin\theta \\ \sin\theta\sin\phi & -\sin\theta\cos\phi & \cos\theta \end{pmatrix} .$$

Note that the order of our rotations was ZXZ. We could have chosen ZYZ instead, or any of XZX, XYX, YXY, and YZY. Any such rotation protocol is referred to as based on *proper Euler angles*. An equivalent system is to adopt one of the following protocols: XYZ, XZY, YZX, YXZ, ZXY, or ZYX, corresponding to the so-called *Tait-Bryan angles*. The latter are used, inter alia, in aeronautics, where they are known respectively as *roll*, *pitch*, and *yaw* (see Fig. 9.7).

Gimbal locking

A *gimbal* is a ring which rotates about a fixed axis. In a gyroscope, the inner rotor typically rotates at a very high angular velocity such that its spin axis is fixed in an inertial frame. The orientation of the

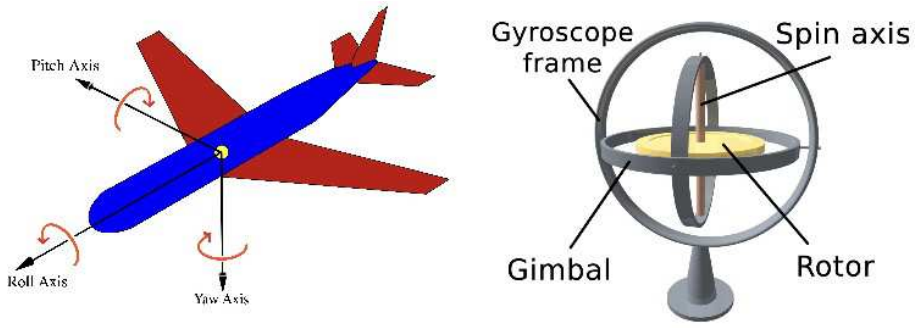

Figure 9.7: Left: Roll, pitch, and yaw. Right: A gyroscope with two gimbals. If the gyroscope frame is free to rotate about its axis, this serves as a third gimbal. *(Image credits: Wikipedia)*

gimbal axes in an *inertial measurement unit* (IMU) may then be used to determine attitude and angular velocity. Replacing the rotor with a camera, the gimbals can be rotated to achieve a desired orientation, say for tracking an object as it moves in three-dimensional space.

A problem arises, though, when the orientation of an object is described using the Euler angles. This is illustrated in Eqn. 9.62 when the angle θ is set to zero, in which case

$$\mathcal{R}(\phi, \theta = 0, \psi) = \begin{pmatrix} \cos(\phi+\psi) & \sin(\phi+\psi) & 0 \\ -\sin(\phi+\psi) & \cos(\phi+\psi) & 0 \\ 0 & 0 & 1 \end{pmatrix} \quad . \tag{9.63}$$

We would expect that fixing one of the Euler angles would still allow us to independently rotate about two remaining axes, but we see above that when $\theta = 0$, the space of rotation matrices becomes one-dimensional! A similar problem occurs when $\theta = \pi$, where

$$\mathcal{R}(\phi, \theta = \pi, \psi) = \begin{pmatrix} \cos(\phi-\psi) & \sin(\phi-\psi) & 0 \\ \sin(\phi-\psi) & -\cos(\phi-\psi) & 0 \\ 0 & 0 & -1 \end{pmatrix} \quad . \tag{9.64}$$

Thus, the two-dimensional space of points (ϕ, ψ) maps to a *one*-dimensional subset of $\mathsf{SO}(3)$. You might wonder whether the problem goes away if we choose Tait-Bryan angles instead. It doesn't.

What we are encountering here is a *coordinate singularity* associated with the way we are coordinatizing the $\mathsf{SO}(3)$ manifold[2]. Something analogous happens when we coordinatize the two-sphere S^2 using polar (θ) and azimuthal (ϕ) angles. Precisely at the poles $\theta = 0$ and $\theta = \pi$, the all azimuthal angles ϕ map to the same point, and we have a zero-dimensional rather than a one-dimensional space. In the context of Euler angles, this coordinate singularity is referred to as *gimbal lock*. Navigational difficulties associated with gimbal lock can be avoided by adding a redundant fourth gimbal to an IMU[3], which can be cumbersome, or by using different coordinates on $\mathsf{SO}(3)$, such as *unit quaternions*.

[2] $\mathsf{SO}(3)$ is a *Lie group*, meaning that it is a manifold with a group structure such that the group operations of multiplication and inverse are smooth.

[3] About two hours after the Apollo 11 moon landing on July 20, 1969, NASA Mission Control in Houston contacted Command Module pilot Michael Collins to inform him that he was "maneuvering very close to gimbal lock" and suggesting he back away, whereupon Collins replied saying that he was trying to avoid this situation, adding wryly, "How about sending me a fourth gimbal for Christmas?"

9.6.2 Precession, nutation, and axial rotation

Next, we'd like to relate the components $\omega_\mu = \boldsymbol{\omega} \cdot \hat{\mathbf{e}}_\mu$ (with $\hat{\mathbf{e}}_\mu \equiv \hat{\mathbf{e}}'''_\mu$) of the rotation in the body-fixed frame to the derivatives $\dot\phi$, $\dot\theta$, and $\dot\psi$. To do this, we write

$$\boldsymbol{\omega} = \dot\phi\,\hat{\mathbf{e}}_\phi + \dot\theta\,\hat{\mathbf{e}}_\theta + \dot\psi\,\hat{\mathbf{e}}_\psi \quad , \tag{9.65}$$

where

$$\begin{aligned} \hat{\mathbf{e}}^0_3 = \hat{\mathbf{e}}_\phi &= \sin\theta\sin\psi\,\hat{\mathbf{e}}_1 + \sin\theta\cos\psi\,\hat{\mathbf{e}}_2 + \cos\theta\,\hat{\mathbf{e}}_3 \\ \hat{\mathbf{e}}_\theta &= \cos\psi\,\hat{\mathbf{e}}_1 - \sin\psi\,\hat{\mathbf{e}}_2 \qquad (\text{“line of nodes”}) \\ \hat{\mathbf{e}}_\psi &= \hat{\mathbf{e}}_3 \quad . \end{aligned} \tag{9.66}$$

The first of these follows from the relation $\hat{\mathbf{e}}_\mu = \mathcal{R}_{\mu\nu}(\phi,\theta,\psi)\,\hat{\mathbf{e}}^0_\nu$, whose inverse is $\hat{\mathbf{e}}^0_\mu = \mathcal{R}^{\rm t}_{\mu\nu}(\phi,\theta,\psi)\,\hat{\mathbf{e}}_\nu$, since $\mathcal{R}^{-1} = \mathcal{R}^{\rm t}$. Thus the coefficients of $\hat{\mathbf{e}}_{1,2,3}$ in $\hat{\mathbf{e}}^0_3$ are the elements of the rightmost ($\nu = 3$) *column* of $\mathcal{R}(\phi,\theta,\psi)$. We may now read off

$$\begin{aligned} \omega_1 &= \boldsymbol{\omega}\cdot\hat{\mathbf{e}}_1 = \dot\phi\,\sin\theta\sin\psi + \dot\theta\cos\psi \\ \omega_2 &= \boldsymbol{\omega}\cdot\hat{\mathbf{e}}_2 = \dot\phi\,\sin\theta\cos\psi - \dot\theta\,\sin\psi \\ \omega_3 &= \boldsymbol{\omega}\cdot\hat{\mathbf{e}}_3 = \dot\phi\cos\theta + \dot\psi \quad . \end{aligned} \tag{9.67}$$

Note that

$$\dot\phi \leftrightarrow \text{precession} \quad , \quad \dot\theta \leftrightarrow \text{nutation} \quad , \quad \dot\psi \leftrightarrow \text{axial rotation} \quad . \tag{9.68}$$

The general form of the kinetic energy is then

$$T = \tfrac{1}{2}I_1\big(\dot\phi\,\sin\theta\sin\psi + \dot\theta\cos\psi\big)^2 + \tfrac{1}{2}I_2\,\big(\dot\phi\,\sin\theta\cos\psi - \dot\theta\,\sin\psi\big)^2 + \tfrac{1}{2}I_3\,\big(\dot\phi\cos\theta + \dot\psi\big)^2 \quad .$$

Note that

$$\boldsymbol{L} = p_\phi\,\hat{\mathbf{e}}_\phi + p_\theta\,\hat{\mathbf{e}}_\theta + p_\psi\,\hat{\mathbf{e}}_\psi \quad , \tag{9.69}$$

which may be verified by explicit computation.

9.6.3 Torque-free symmetric top

A body falling in a gravitational field experiences no net torque about its CM:

$$\boldsymbol{N}^{\rm ext} = \sum_i \boldsymbol{r}_i \times (-m_i\,\boldsymbol{g}) = \boldsymbol{g}\times\sum_i m_i\,\boldsymbol{r}_i = 0 \quad . \tag{9.70}$$

For a symmetric top with $I_1 = I_2$, we have

$$T = \tfrac{1}{2}I_1\big(\dot\theta^2 + \dot\phi^2\,\sin^2\theta\big) + \tfrac{1}{2}I_3\big(\dot\phi\cos\theta + \dot\psi\big)^2 \quad . \tag{9.71}$$

The potential is cyclic in the Euler angles, hence the equations of motion are

$$\frac{d}{dt}\,\frac{\partial T}{\partial(\dot\phi,\dot\theta,\dot\psi)} = \frac{\partial T}{\partial(\phi,\theta,\psi)} \quad . \tag{9.72}$$

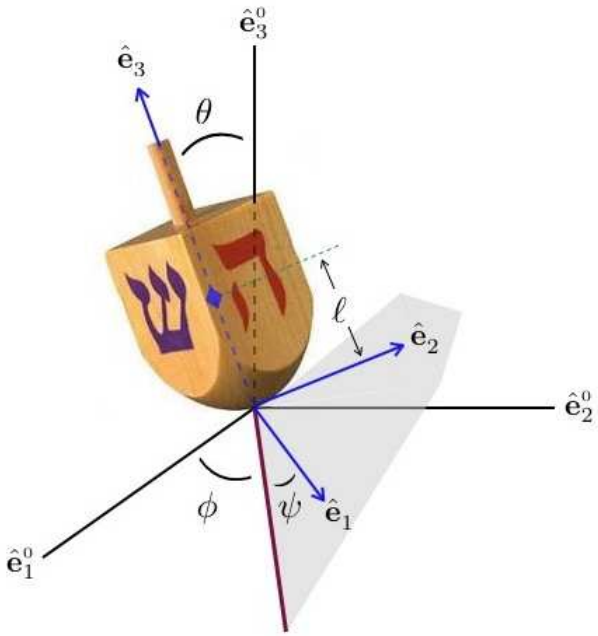

Figure 9.8: A *dreidl* is a symmetric top. The four-fold symmetry axis guarantees $I_1 = I_2$. The blue diamond represents the center-of-mass and lies within the object.

Since ϕ and ψ are cyclic in T, their conjugate momenta are conserved:

$$\begin{aligned} p_\phi &= \frac{\partial L}{\partial \dot\phi} = I_1\,\dot\phi\,\sin^2\theta + I_3\,(\dot\phi\cos\theta + \dot\psi)\,\cos\theta \\ p_\psi &= \frac{\partial L}{\partial \dot\psi} = I_3\,(\dot\phi\cos\theta + \dot\psi) \quad . \end{aligned} \tag{9.73}$$

Note that $p_\psi = I_3\,\omega_3$, hence ω_3 is constant, as we have already seen.

To solve for the motion, we first note that $\boldsymbol{L}$ is conserved in the inertial frame. We are therefore permitted to define $\hat{\boldsymbol{L}} = \hat{\mathbf{e}}_3^0 = \hat{\mathbf{e}}_\phi$. Thus, $p_\phi = L$. Since $\hat{\mathbf{e}}_\phi \cdot \hat{\mathbf{e}}_\psi = \cos\theta$, we have that $p_\psi = \boldsymbol{L}\cdot\hat{\mathbf{e}}_\psi = L\cos\theta$. Finally, $\hat{\mathbf{e}}_\phi \cdot \hat{\mathbf{e}}_\theta = 0$, which means $p_\theta = \boldsymbol{L}\cdot\hat{\mathbf{e}}_\theta = 0$. From the equations of motion,

$$\dot p_\theta = I_1\,\ddot\theta = \big(I_1\,\dot\phi\cos\theta - p_\psi\big)\,\dot\phi\sin\theta \quad , \tag{9.74}$$

hence we must have

$$\dot\theta = 0 \quad , \quad \dot\phi = \frac{p_\psi}{I_1\cos\theta} \quad . \tag{9.75}$$

Note that $\dot\theta = 0$ follows from conservation of $p_\psi = L\cos\theta$. From the equation for p_ψ, we may now conclude

$$\dot\psi = \frac{p_\psi}{I_3} - \frac{p_\psi}{I_1} = \left(\frac{I_3 - I_1}{I_3}\right)\omega_3 \quad , \tag{9.76}$$

which recapitulates (9.44), with $\dot\psi = \Omega$.

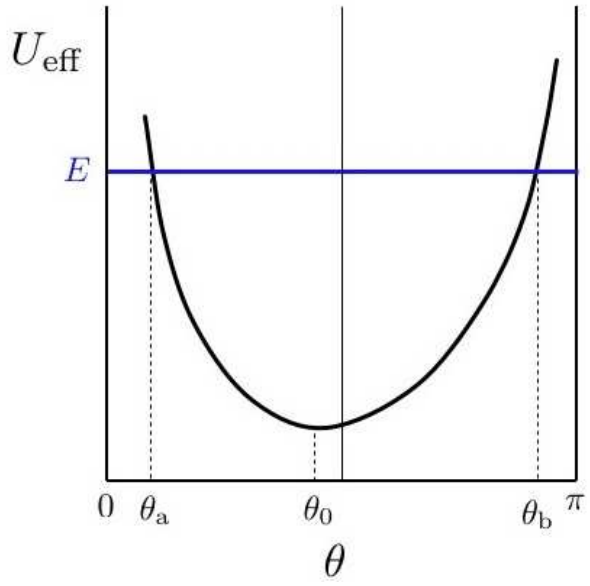

Figure 9.9: The effective potential of eq. 9.85.

9.6.4 Symmetric top with one point fixed

Consider the case of a symmetric top with one point fixed, as depicted in fig. 9.8. The Lagrangian is

$$L = \tfrac{1}{2} I_1 \big(\dot\theta^2 + \dot\phi^2 \, \sin^2\theta\big) + \tfrac{1}{2} I_3 \big(\dot\phi \cos\theta + \dot\psi\big)^2 - Mg\ell \cos\theta \quad . \tag{9.77}$$

Here, ℓ is the distance from the fixed point to the CM, and the inertia tensor is defined along principal axes whose origin lies at the fixed point (not the CM!). Gravity now supplies a torque, but as in the torque-free case, the Lagrangian is still cyclic in ϕ and ψ, so

$$\begin{aligned} p_\phi &= (I_1 \sin^2\theta + I_3 \cos^2\theta)\,\dot\phi + I_3 \cos\theta\,\dot\psi \\ p_\psi &= I_3 \cos\theta\,\dot\phi + I_3\,\dot\psi \end{aligned} \tag{9.78}$$

are each conserved. We can invert these relations to obtain $\dot\phi$ and $\dot\psi$ in terms of $\{p_\phi, p_\psi, \theta\}$:

$$\dot\phi = \frac{p_\phi - p_\psi \, \cos\theta}{I_1 \, \sin^2\theta} \quad , \quad \dot\psi = \frac{p_\psi}{I_3} - \frac{(p_\phi - p_\psi \, \cos\theta) \, \cos\theta}{I_1 \, \sin^2\theta} \quad . \tag{9.79}$$

In addition, since $\partial L/\partial t = 0$, the total energy is conserved:

$$E = T + U = \tfrac{1}{2} I_1 \, \dot\theta^2 + \overbrace{\frac{(p_\phi - p_\psi \, \cos\theta)^2}{2I_1 \, \sin^2\theta} + \frac{p_\psi^2}{2I_3} + Mg\ell \cos\theta}^{U_{\rm eff}(\theta)} \quad , \tag{9.80}$$

where the term under the brace is the effective potential $U_{\rm eff}(\theta)$.

The problem thus reduces to the one-dimensional dynamics of $\theta(t)$, *i.e.*

$$I_1 \, \ddot\theta = -\frac{\partial U_{\rm eff}}{\partial \theta} \quad , \tag{9.81}$$

with

$$U_{\rm eff}(\theta) = \frac{(p_\phi - p_\psi\,\cos\theta)^2}{2I_1\,\sin^2\theta} + \frac{p_\psi^2}{2I_3} + Mg\ell\cos\theta \quad . \tag{9.82}$$

Using energy conservation, we may write

$$dt = \pm\sqrt{\frac{I_1}{2}}\,\frac{d\theta}{\sqrt{E - U_{\rm eff}(\theta)}} \quad . \tag{9.83}$$

and thus the problem is reduced to quadratures:

$$t(\theta) = t(\theta_0) \pm \sqrt{\frac{I_1}{2}}\int\limits_{\theta_0}^{\theta} d\vartheta\,\frac{1}{\sqrt{E - U_{\rm eff}(\vartheta)}} \quad . \tag{9.84}$$

We can gain physical insight into the motion by examining the shape of the effective potential,

$$U_{\rm eff}(\theta) = \frac{(p_\phi - p_\psi\,\cos\theta)^2}{2I_1\,\sin^2\theta} + Mg\ell\cos\theta + \frac{p_\psi^2}{2I_3} \quad , \tag{9.85}$$

over the interval $\theta \in [0,\pi]$. Clearly $U_{\rm eff}(0) = U_{\rm eff}(\pi) = \infty$, so the motion must be bounded. What is not yet clear, but what is nonetheless revealed by some additional analysis, is that $U_{\rm eff}(\theta)$ has a single minimum on this interval, at $\theta = \theta_0$. The turning points for the θ motion are at $\theta = \theta_{\rm a}$ and $\theta = \theta_{\rm b}$, where $U_{\rm eff}(\theta_{\rm a}) = U_{\rm eff}(\theta_{\rm b}) = E$. Clearly if we expand about θ_0 and write $\theta = \theta_0 + \eta$, the η motion will be harmonic, with

$$\eta(t) = \eta_0\,\cos(\Omega t + \delta) \quad , \quad \Omega = \sqrt{\frac{U_{\rm eff}''(\theta_0)}{I_1}} \quad . \tag{9.86}$$

To prove that $U_{\rm eff}(\theta)$ has these features, let us define $u \equiv \cos\theta$. Then $\dot u = -\dot\theta\,\sin\theta$, and from $E = \frac{1}{2}I_1\,\dot\theta^2 + U_{\rm eff}(\theta)$ we derive

$$\dot u^2 = \left(\frac{2E}{I_1} - \frac{p_\psi^2}{I_1 I_3}\right)(1-u^2) - \frac{2Mg\ell}{I_1}\,(1-u^2)\,u - \left(\frac{p_\phi - p_\psi\,u}{I_1}\right)^2 \equiv f(u) \quad . \tag{9.87}$$

The turning points occur at $f(u) = 0$. The function $f(u)$ is cubic, and the coefficient of the cubic term is $2Mg\ell/I_1$, which is positive. Clearly $f(u = \pm 1) = -(p_\phi \mp p_\psi)^2/I_1^2$ is negative, so there must be at least one solution to $f(u) = 0$ on the interval $u \in (1,\infty)$. Clearly there can be at most three real roots for $f(u)$, since the function is cubic in u, hence there are at most two turning points on the interval $u \in [-1,1]$. Thus, $U_{\rm eff}(\theta)$ has the form depicted in fig. 9.9.

To apprehend the full motion of the top in an inertial frame, let us follow the symmetry axis $\hat{\mathbf{e}}_3$:

$$\hat{\mathbf{e}}_3 = \sin\theta\sin\phi\,\hat{\mathbf{e}}_1^0 - \sin\theta\cos\phi\,\hat{\mathbf{e}}_2^0 + \cos\theta\,\hat{\mathbf{e}}_3^0 \quad . \tag{9.88}$$

Once we know $\theta(t)$ and $\phi(t)$ we're done. The motion $\theta(t)$ is described above: θ oscillates between turning points at $\theta_{\rm a}$ and $\theta_{\rm b}$. As for $\phi(t)$, we have already derived the result

$$\dot\phi = \frac{p_\phi - p_\psi\,\cos\theta}{I_1\,\sin^2\theta} \quad . \tag{9.89}$$

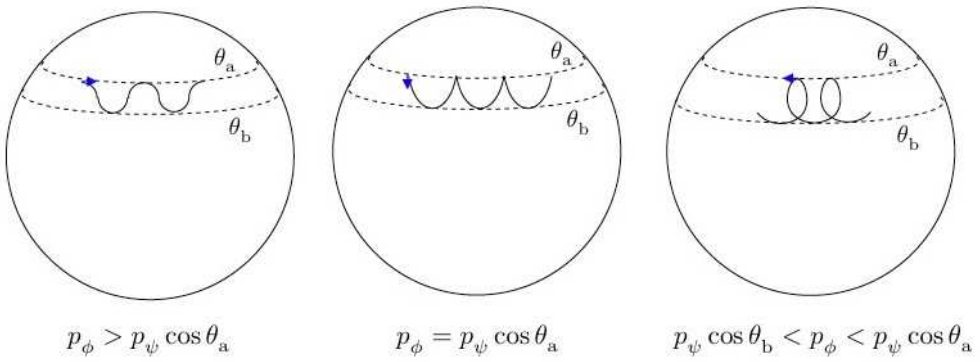

Figure 9.10: Precession and nutation of the symmetry axis of a symmetric top.

Thus, if $p_\phi > p_\psi \cos\theta_a$, then $\dot\phi$ will remain positive throughout the motion. If, on the other hand, we have

$$p_\psi \cos\theta_b < p_\phi < p_\psi \cos\theta_a \quad , \tag{9.90}$$

then $\dot\phi$ changes sign at an angle $\theta^* = \cos^{-1}\left(p_\phi/p_\psi\right)$. The motion is depicted in fig. 9.10. An extensive discussion of this problem is given in H. Goldstein, *Classical Mechanics*.

9.7 Rolling and Skidding Motion of Real Tops

The material in this section is based on the corresponding sections from V. Barger and M. Olsson, *Classical Mechanics: A Modern Perspective*. This is an excellent book which contains many interesting applications and examples.

9.7.1 Rolling tops

In most tops, the point of contact rolls or skids along the surface. Consider the peg end top of fig. 9.11, executing a circular rolling motion, as sketched in fig. 9.12. There are three components to the force acting on the top: gravity, the normal force from the surface, and friction. The frictional force is perpendicular to the CM velocity, and results in centripetal acceleration of the top:

$$f = M\Omega^2\rho \le \mu Mg \quad , \tag{9.91}$$

where Ω is the frequency of the CM motion and μ is the coefficient of friction. If the above inequality is violated, the top starts to slip.

The frictional and normal forces combine to produce a torque $N = Mg\ell\sin\theta - f\ell\cos\theta$ about the CM[4]. This torque is tangent to the circular path of the CM, and causes $\boldsymbol{L}$ to precess. We assume that the top is spinning rapidly, so that $\boldsymbol{L}$ very nearly points along the symmetry axis of the top itself. (As we'll see, this

[4]Gravity of course produces no net torque about the CM.

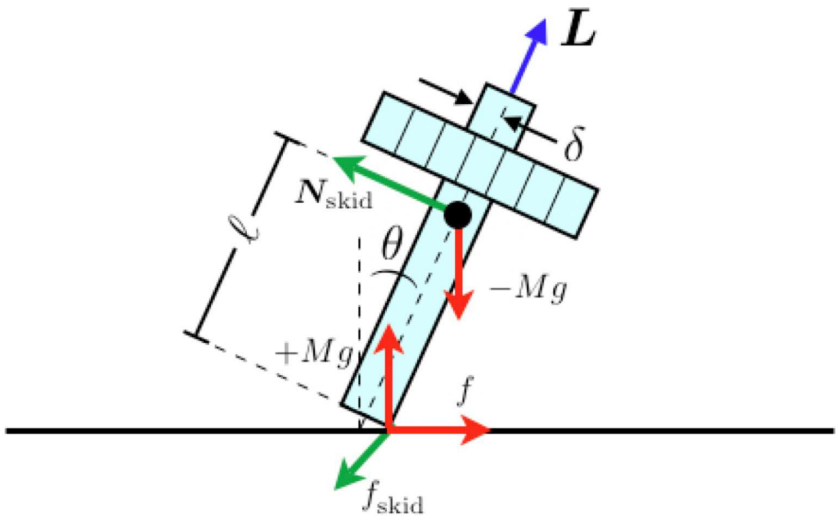

Figure 9.11: A top with a peg end. The frictional forces $\boldsymbol{f}$ and $\boldsymbol{f}_{\rm skid}$ are shown. When the top rolls without skidding, $\boldsymbol{f}_{\rm skid} = 0$.

is true for slow precession but not for fast precession, where the precession frequency is proportional to ω_3.) The precession is then governed by the equation

$$\begin{aligned} N &= Mg\ell\sin\theta - f\ell\cos\theta \\ &= \left|\dot{\boldsymbol{L}}\right| = \left|\boldsymbol{\Omega}\times\boldsymbol{L}\right| \approx \Omega\, I_3\,\omega_3\sin\theta \quad , \end{aligned} \tag{9.92}$$

where $\hat{\mathbf{e}}_3$ is the instantaneous symmetry axis of the top. Substituting $f = M\Omega^2\rho$,

$$\frac{Mg\ell}{I_3\,\omega_3}\left(1 - \frac{\Omega^2\rho}{g}\,\mathrm{ctn}\,\theta\right) = \Omega \quad , \tag{9.93}$$

which is a quadratic equation for Ω. We supplement this with the 'no slip' condition,

$$\omega_3\,\delta = \Omega\left(\rho + \ell\sin\theta\right) \quad , \tag{9.94}$$

resulting in two equations for the two unknowns Ω and ρ.

Substituting for $\rho(\Omega)$ and solving for Ω, we obtain

$$\Omega = \frac{I_3\,\omega_3}{2M\ell^2\cos\theta}\left\{1 + \frac{Mg\ell\delta}{I_3}\,\mathrm{ctn}\,\theta \pm \sqrt{\left(1 + \frac{Mg\ell\delta}{I_3}\,\mathrm{ctn}\,\theta\right)^2 - \frac{4M\ell^2}{I_3}\cdot\frac{Mg\ell}{I_3\,\omega_3^2}}\right\} \quad . \tag{9.95}$$

This in order to have a real solution we must have

$$\omega_3 \geq \frac{2M\ell^2\sin\theta}{I_3\sin\theta + Mg\ell\delta\cos\theta}\sqrt{\frac{g}{\ell}} \quad . \tag{9.96}$$

If the inequality is satisfied, there are two possible solutions for Ω, corresponding to fast and slow precession. Usually one observes slow precession. Note that it is possible that $\rho < 0$, in which case the CM and the peg end lie on opposite sides of a circle from each other.

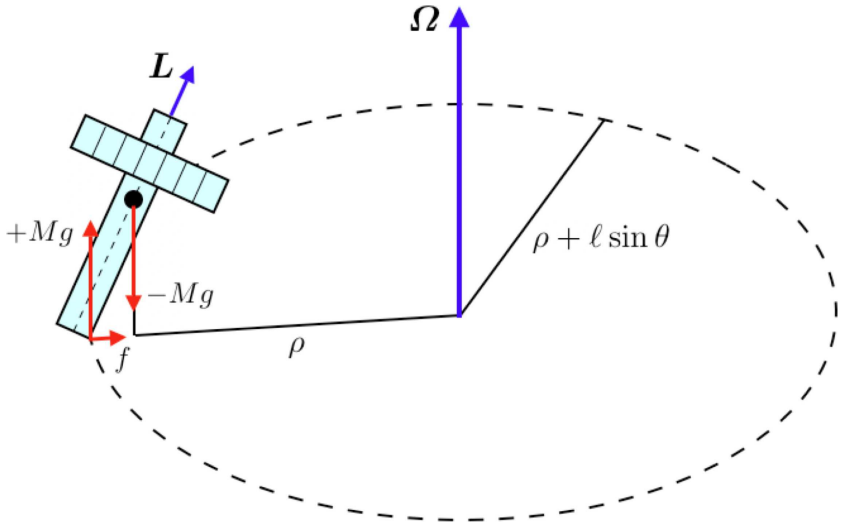

Figure 9.12: Circular rolling motion of the peg top.

9.7.2 Skidding tops

A skidding top experiences a frictional force which opposes the skidding velocity, until $v_{\rm skid} = 0$ and a pure rolling motion sets in. This force provides a torque which makes the top *rise:*

$$\dot\theta = -\frac{N_{\rm skid}}{L} = -\frac{\mu M g \ell}{I_3\,\omega_3} \quad . \tag{9.97}$$

Suppose $\delta \approx 0$, in which case $\rho + \ell\sin\theta = 0$, from eqn. 9.94, and the point of contact remains fixed. Now recall the effective potential for a symmetric top with one point fixed:

$$U_{\rm eff}(\theta) = \frac{(p_\phi - p_\psi\,\cos\theta)^2}{2I_1\,\sin^2\theta} + \frac{p_\psi^2}{2I_3} + Mg\ell\cos\theta \quad . \tag{9.98}$$

We demand $U'_{\rm eff}(\theta_0) = 0$, which yields

$$\cos\theta_0\cdot\beta^2 - p_\psi\sin^2\theta_0\cdot\beta + Mg\ell I_1\sin^4\theta_0 = 0 \quad , \tag{9.99}$$

where

$$\beta \equiv p_\phi - p_\psi\cos\theta_0 = I_1\sin^2\theta_0\,\dot\phi \quad . \tag{9.100}$$

Solving the quadratic equation for β, we find

$$\dot\phi = \frac{I_3\,\omega_3}{2I_1\cos\theta_0}\left(1 \pm \sqrt{1 - \frac{4Mg\ell I_1\cos\theta_0}{I_3^2\,\omega_3^2}}\right) \quad . \tag{9.101}$$

This is simply a recapitulation of eqn. 9.95, with $\delta = 0$ and with $M\ell^2$ replaced by I_1. Note $I_1 = M\ell^2$ by the parallel axis theorem if $I_1^{\rm CM} = 0$. But to the extent that $I_1^{\rm CM} \neq 0$, our treatment of the peg top was incorrect. It turns out to be OK, however, if the precession is slow, *i.e.* if $\Omega/\omega_3 \ll 1$.

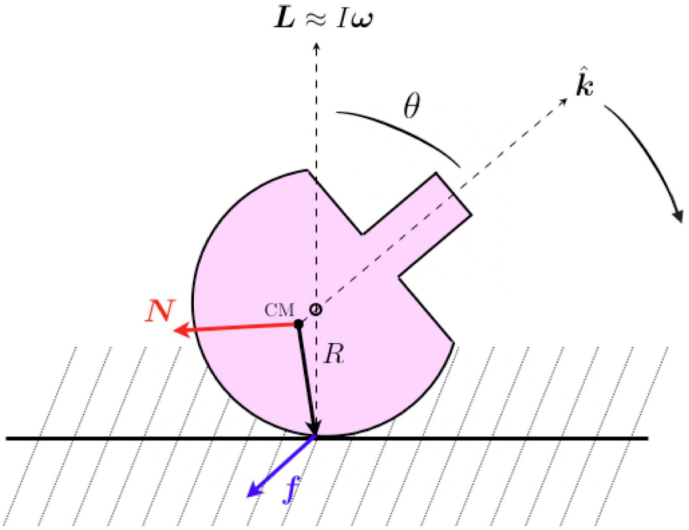

Figure 9.13: The tippie-top behaves in a counterintuitive way. Once started spinning with the peg end up, the peg axis rotates downward. Eventually the peg scrapes the surface and the top rises to the vertical in an inverted orientation.

On a level surface, $\cos\theta_0 > 0$, and therefore we must have

$$\omega_3 \geq \frac{2}{I_3}\sqrt{Mg\ell I_1 \cos\theta_0} \quad . \tag{9.102}$$

Thus, if the top spins too slowly, it cannot maintain precession. Eqn. 9.101 says that there are two possible precession frequencies. When ω_3 is large, we have

$$\dot\phi_{\rm slow} = \frac{Mg\ell}{I_3\,\omega_3} + \mathcal{O}(\omega_3^{-1}) \qquad , \qquad \dot\phi_{\rm fast} = \frac{I_3\,\omega_3}{I_1\cos\theta_0} + \mathcal{O}(\omega_3^{-3}) \quad . \tag{9.103}$$

Again, one usually observes slow precession.

A top with $\omega_3 > \frac{2}{I_3}\sqrt{Mg\ell I_1}$ may 'sleep' in the vertical position with $\theta_0 = 0$. Due to the constant action of frictional forces, ω_3 will eventually drop below this value, at which time the vertical position is no longer stable. The top continues to slow down and eventually falls.

9.7.3 Tippie-top

A particularly nice example from the Barger and Olsson book is that of the tippie-top, a truncated sphere with a peg end, sketched in fig. 9.13 The CM is close to the center of curvature, which means that there is almost no gravitational torque acting on the top. The frictional force $\boldsymbol{f}$ opposes slipping, but as the top spins $\boldsymbol{f}$ rotates with it, and hence the time-averaged frictional force $\langle \boldsymbol{f} \rangle \approx 0$ has almost no effect on the motion of the CM. A similar argument shows that the frictional torque, which is nearly horizontal, also time averages to zero:

$$\left\langle \frac{d\boldsymbol{L}}{dt} \right\rangle_{\rm inertial} \approx 0 \quad . \tag{9.104}$$

In the *body*-fixed frame, however, $\boldsymbol{N}$ is roughly constant, with magnitude $N \approx \mu M g R$, where R is the radius of curvature and μ the coefficient of sliding friction. Now we invoke

$$\boldsymbol{N} = \left.\frac{d\boldsymbol{L}}{dt}\right|_{\rm body} + \ \boldsymbol{\omega} \times \boldsymbol{L} \quad . \tag{9.105}$$

The second term on the RHS is very small, because the tippie-top is almost spherical, hence inertia tensor is very nearly diagonal, and this means

$$\boldsymbol{\omega} \times \boldsymbol{L} \approx \boldsymbol{\omega} \times I\boldsymbol{\omega} = 0 \quad . \tag{9.106}$$

Thus, $\dot{\boldsymbol{L}}_{\rm body} \approx \boldsymbol{N}$, and taking the dot product of this equation with the unit vector $\hat{\boldsymbol{k}}$, we obtain

$$-\,N \sin\theta = \hat{\boldsymbol{k}} \cdot \boldsymbol{N} = \frac{d}{dt}\Big(\hat{\boldsymbol{k}} \cdot \boldsymbol{L}_{\rm body}\Big) = -L \sin\theta\,\dot\theta \quad . \tag{9.107}$$

Thus,

$$\dot\theta = \frac{N}{L} \approx \frac{\mu M g R}{I\omega} \quad . \tag{9.108}$$

Once the stem scrapes the table, the tippie-top rises to the vertical just like any other rising top.